Hot Compression Deformation Behavior of the Mg-5Sn-2.5Pb Magnesium Alloy

Pin XIE[1,a], Yun-Peng ZHU[1,b,*], Pei-Peng JIN[1,c]

[1]Qinghai provincial Key Laboratory of New Light Alloys, Qinghai University, Xining 810016, PR China

[a]xiepin213411@163.com, [b]zyphb2012@live.cn, [c]jingpeipeng@hotmail.com

*Corresponding author

Keywords: Mg-5Sn-2.5Pb Magnesium Alloy, Hot Compression Behavior, Constitutive Equations.

Abstract. Compressive deformation behavior of Mg-5Sn-2.5Pb magnesium alloy was investigated at the temperature range from 250 to 450 ℃, strain rate range from 0.001 to 10s^{-1} and the maximum deformation degree of 60% on Gleeble-3500 thermal simulator. The constitutive equations were established by taking peak stresses as the function of temperatures and strain rates. The results show that the flow stress significantly affected by deformation temperature and strain rate, and the flow stress decreases with the increase of deformation temperature and the decrease of strain rate. The deformation activation energy and stress exponent were evaluated by the hyperbolic-sine mathematics model and the hot deformation constitutive equation was established.

Introduction

The low density, high specific strength and favorable recycling capability of magnesium alloys are particularly suitable for lightweight applications such as in the fields of automotive, aircraft industries, and electronic products [1-2]. However, their ductility and formability are very poor at room temperature due to their hexagonal close-packed crystal structure and the limited number of activated slip systems [3-7]. It limits the plastic forming domain of magnesium alloys. The constitutive equation contains deformation temperature, flow stress and strain rate to describe the mechanical behavior of the material during the forming process.

In this paper, hot compressive tests of Mg-5Sn-2.5Pb magnesium alloy were conducted at different temperatures and strain rates to characterize the flow behavior of the alloy during hot deformation. The constitutive relationship was established with the experimental data. The activation energy and stress exponent of the magnesium alloy during hot deformation were calculated to provide guidance to the reasonable development of hot deformation processing technology of Mg-5Sn-2.5Pb magnesium alloy, such as extrusion and rolling et al.

Experimental

The ingot of the fabricated magnesium alloy were machined to cylindrical specimens with dimension of Φ10mm×15mm. Hot compressive tests were conducted with Gleeble-3500 thermal simulator at a temperature range of 250 ℃ to 450 ℃ and intervals of 50 ℃. Five typical strain rates were chosen from 0.001 to 10s^{-1}. The temperature was controlled and measured with a thermocouple welded to the sample at mid-height. The samples were compressed evenly on both ends of the lubricant and graphite samples in order to reduce the friction between sample and the ends of the indenter. The samples were heated to the deformation temperature at a heating rate of 5 ℃/s; then held 1 min to homogenize the temperature in the sample and subsequently deformed up to a true strain of 0.6, and then water quenched immediately after deformation in order to preserve the thermal deformation texture.

Results and Discussion

True Stress-strain Relationships

The true stress-strain curves of Mg-5Sn-2.5Pb magnesium alloy are presented in Fig.1. A similar phenomenon can be observed in true stress-strain curves of the other alloys [8-11]. The flow stress increase to a peak at a relatively low strain due to the forming mechanism dominated by work hardening. Then in the subsequently deformation period, the stress decrease as a result of dynamic recrystallization (DRX) which overtakes initial work hardening. The stress reach to a steady state is mainly attributed to work hardening and softening reach a dynamic equilibrium, the dislocation density remains relatively constant, the softening phenomenon is due to the dynamic recovery (DRV) and dynamic recrystallization (DRX) [8, 12-13]. The flow stress significantly affected by strain rate and deformation temperature[12-14]. The peak stress decreases with the increasing of deformation temperature and the decreasing of strain rate, as shown in Fig.2.

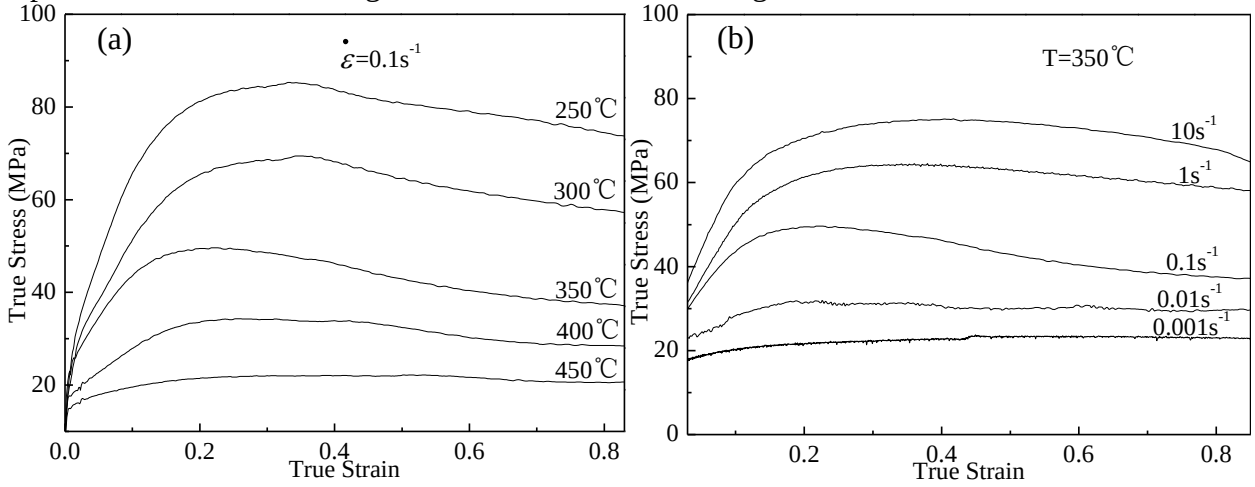

Fig.1 True stress-strain curves of the alloy at different deformation conditions: (a) $\dot{\varepsilon}$ =0.1s^{-1} and (b) 350 ℃

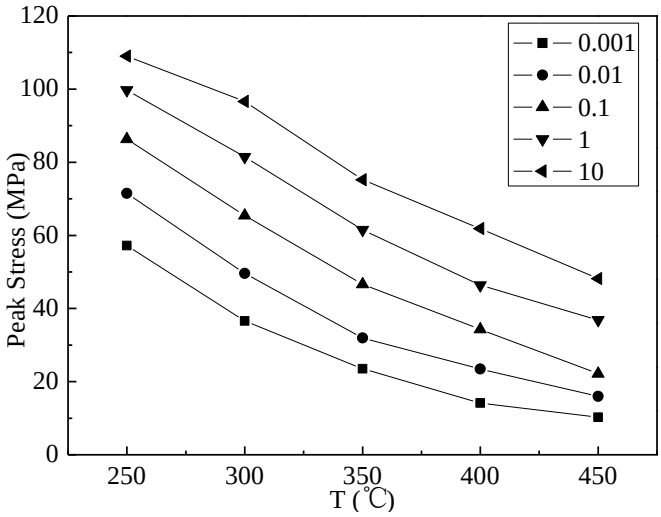

Fig.2 Peak Stress at varied temperatures

Constitutive Equations

Various constitutive equations have been used to describe the stress-strain relationship of hot deformed alloys. The Arrhenius equation has been widely used to describe the stress-strain relationship, especially at a wide range of temperature and strain rate [14-16]. Therefore, in the present study the Arrhenius equation (1) was employed to analyze the hot deformation behaviors of Mg-5Sn-2.5Pb magnesium alloy.

$$\dot{\varepsilon} = A[\sinh(\alpha\sigma)]^n \exp(-\frac{Q}{RT}) \quad (1)$$

$$Z = \dot{\varepsilon} \exp(-\frac{Q}{RT}) \quad (2)$$

$$Q = R\left[\frac{\partial \ln(\sinh(\alpha\sigma))}{\partial(1/T)}\right]_{\dot{\varepsilon}}\left[\frac{\partial \ln \dot{\varepsilon}}{\partial \ln(\sinh(\alpha\sigma))}\right]_T \quad (3)$$

Where A, α ($=\beta/n'$) are constants of the material, n is stress exponent, Q is an apparent activation energy of the deformation, R is the gas constant. Z is the Zener–Hollomon parameter, also known as temperature compensated strain rate, which is determined by the strain rate $\dot{\varepsilon}$ and temperature T.

The value Q is calculated from the equation (3), this Q value and the peak stress σ_p as the σ are given in equation (1) and then the values of A and n are obtained from the plot of ln$Z$ versus ln[sinh($\alpha\sigma$)]. The plots of flow stress versus strain rate obtained by filled experimental data are shown in Fig.3. The α value was determined as 0.0208MPa^{-1} by linear regressed the relation between $\ln\dot{\varepsilon}$ -lnσ_p and $\ln\dot{\varepsilon}$ -σ_p at varied temperature.

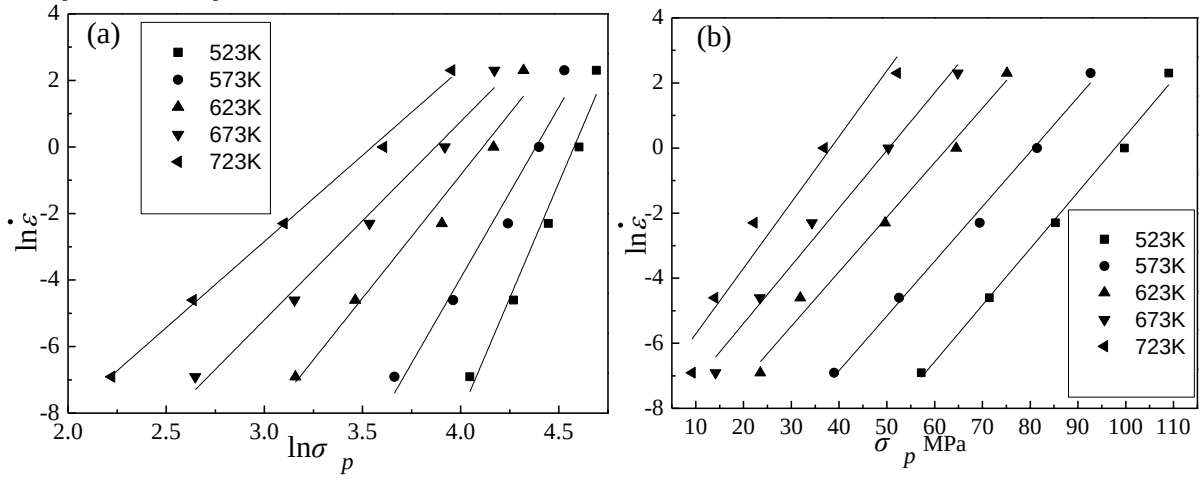

Fig.3 Relationship between $\ln\dot{\varepsilon}$ and $\ln\sigma_p$, $\ln\dot{\varepsilon}$ and σ_p at different temperatures

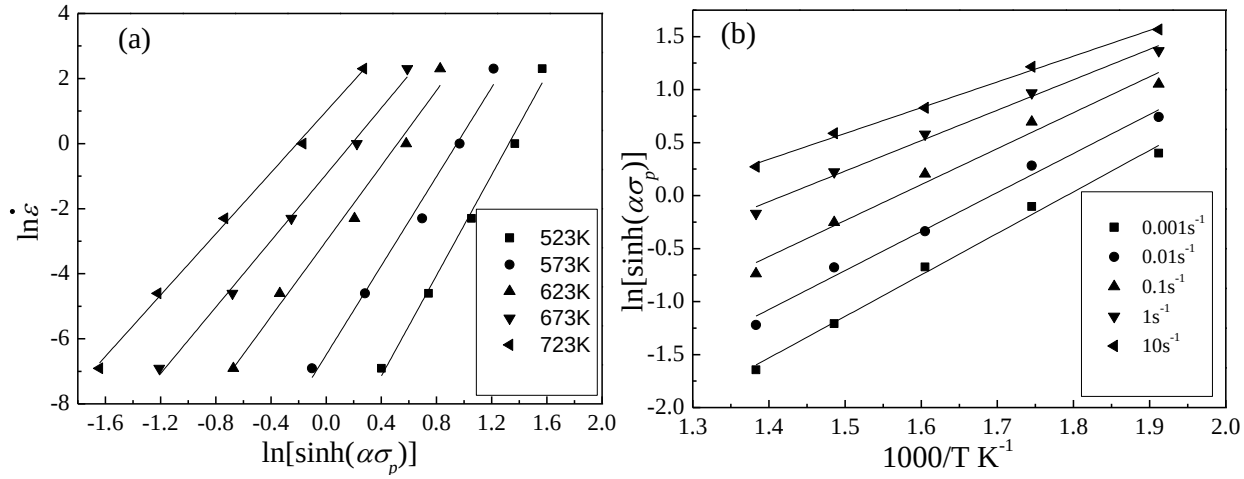

Fig.4 Relationship between $\ln\dot{\varepsilon}$ and ln[sinh($\alpha\sigma_p$)] at different temperatures, ln[sinh($\alpha\sigma_p$)] and 1000/T at various strain rates

The Q is an indicator of deformation difficulty degree in plasticity deformation theory, it can be calculated by Eq. (3). Fig.4 (a) and (b) show $\ln\dot{\varepsilon}$ versus $\ln[\sinh(\alpha\sigma_p)]$ and $\ln[\sinh(\alpha\sigma_p)]$ versus

1000/T. The values of $\left\{\partial \ln \dot{\varepsilon}/\partial \ln\left[\sinh(\alpha\sigma_p)\right]\right\}_T$ and $\left\{\partial \ln\left[\sinh(\alpha\sigma_p)\right]/\partial(1/T)\right\}_{\dot{\varepsilon}}$ can be obtained by linear regression algorithm given in Fig.4. They are determined substituting the slopes of Fig.4 into Eq. (3), and the calculated value of the deformation activity energy is Q=163.7kJ/mol.

By substituting Eq. (2) into Eq. (1) and taking the natural logarithm of both sides, the curve of ln$Z$ vs ln[sinh($\alpha\sigma_p$)] is plotted in Fig.5 by linear regression algorithm. The relationship of ln$Z$ and ln[sinh($\alpha\sigma_p$)] is given in Eq. (4).

$$\ln Z = 28.79 + 5.84 \ln\left[\sinh(\alpha\sigma)\right] \tag{4}$$

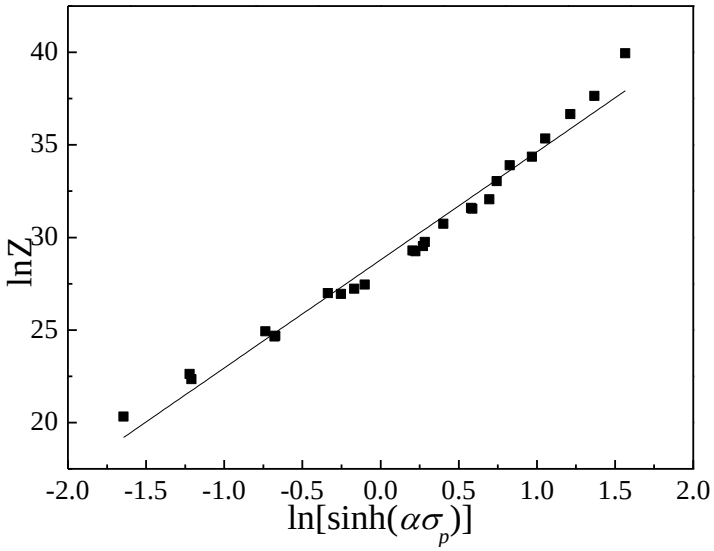

Fig.5 Relationship between ln$Z$ and ln[sinh($\alpha\sigma_p$)]

From Eq. (4), n and A can be obtained. Finally, substituting the values of α, n, A and Q into Eq(1), the plastic flow semi-empirical model for $\dot{\varepsilon}$ and T can be expressed as follows:

$$\dot{\varepsilon} = 3.2187\times10^{12} \ln\left[\sinh(0.0208\sigma)\right]^{5.84} \exp\left(-\frac{163.7}{RT}\right) \tag{5}$$

Fig.6 illustrates the comparison between calculated and measured peak stresses σ_p. It is found that the predicted values and the measured values agree with very well. The maximum relative error is 14.9% at T=250 ℃ and strain rate $\dot{\varepsilon}$=10s^{-1}, the other relative errors are below 5%, and the hyperbolic sine law can be applied over entire stress range for the alloy fabricated in this work .

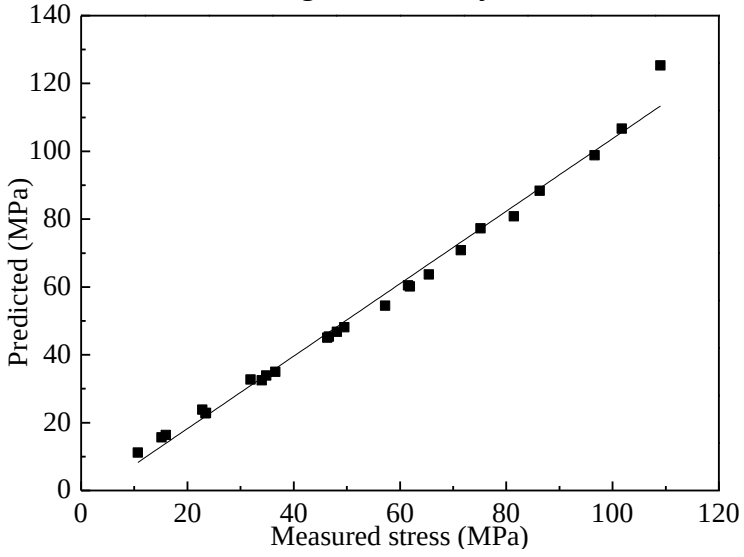

Fig.6 Relationship between calculated and measured σ_p values

Summary

The hot deformation behavior of Mg-5Sn-2.5Pb magnesium alloy has been analyzed by means of isothermal compression at the temperature range from 250 to 450 ℃, strain rate range from 0.001 to $10s^{-1}$. The following conclusions have been drawn:

1. The constitutive equation of Mg-5Sn-2.5Pb magnesium alloy is:

$$\dot{\varepsilon} = 3.2187 \times 10^{12} \ln[\sinh(0.0208\sigma)]^{5.84} \exp\left(-\frac{163.7}{RT}\right)$$

2. The relative errors between predicted values and the measured values are less than 15%.

Acknowledgement

This work was financially supported by Foundation for Middle-aged and young of Qinghai University (2014-QGY-3) and Qinghai Science and Technology Project (2014-ZJ-709).

References

[1] Bin Chen, Wei-Min Zhou, et al. Hot Compression Deformation Behavior and Processing Maps of Mg-Gd-Y-Zr Alloy[J]. Journal of Materials Engineering and Performance, 2013, 22(9): 2458–2466.

[2]C. Dharmendra, K. P. Rao, et al. Hot workability analysis with processing map and texture characteristics of as-cast TX32 magnesium alloy[J]. J Mater Sci, 2013, 48: 5236–5246.

[3] M. Lentz, S. Gall, F. Schmack, et al. Hot working behavior of a WE54 magnesium alloy[J]. J Mater Sci, 2014, 49: 1121–1129.

[4]LI Yongbing, CHEN Yunbo, CUI Hua, et al. Hot deformation behavior of a spray-deposited AZ31 magnesium alloy[J]. Rare Metals, 2009, 28: 91-97.

[5]YU Kun, CAI Zhi-yong, et al. Constitutive analysis of AZ31 magnesium alloy plate[J]. Springer, 2010, 17: 7−12.

[6]Hui Yu, Huashun Yu, Guanghui Min, et al. Strain-Dependent Constitutive Analysis of Hot Deformation and Hot Workability of T4-Treated ZK60 Magnesium Alloy[J]. Met. Mater, 2013, 4(19): 651~665.

[7] M. Lentz, S. Gall, F. Schmack, et al. Hot working behavior of a WE54 magnesium alloy[J]. J Mater Sci , 2014, 49: 1121–1129.

[8]Mingliang Wang, Peipeng Jin and Jinhui Wang. Hot Deformation and Processing Maps of 7005 Aluminum Alloy[J]. High Temp. Mater. Proc, 2014, 33(4): 369-375.

[9]F. A. Slooff , J. Zhou , J. Duszczyk , L. Katgerman. Strain-dependent constitutive analysis of three wrought Mg–Al–Zn alloys[J]. J Mater Sci, 2008, 43: 7165–7170.

[10]H. Y. Li, Y. Liu, X. C. Lu, X. J. Su. Constitutive modeling for hot deformation behavior of ZA27 alloy[J]. J Mater Sci, 2012, 47: 5411–5418.

[11]Yan Lou, Heng Chen, Changxing Ke and Min Long. Hot Tensile Deformation Characteristics and Processing Map of Extruded AZ80 Mg Alloys[J]. Journal of Materials Engineering and Performance, 2014, 23: 1904-1914.

[12]S. Gall, M. Huppmann, H. M. Mayer, S. Muller, W. Reimers. Hot working behavior of AZ31 and ME21 magnesium alloys[J]. J Mater Sci , 2013, 48: 473–480.

[13]LI Bo, PAN Qing-lin, LI Chen, et al. Hot compressive deformation behavior and constitutive relationship of Al-Zn-Mg-Zr alloy with trace amounts of Sc[J]. Springer, 2013, 20: 2939−2946.

[14]Yunpeng Zhu, Peipeng Jin, et al. Hot deformation behavior of Mg2B2O5 whiskers reinforced AZ31B magnesium composite fabricated by stir-casting[J]. Materials Science & Engineering A, 2013, 573: 148-153.

[15]ZHANG Kui, MA Minglong, LI Xinggang, et al. Hot deformation behavior of Mg-7.22Gd-4.84Y-1.26Nd-0.58Zr magnesium alloy[J]. Rare Metals, 2011, 1(30): 87-93.

[16]Hui Yu, Huashun Yu, et al. Strain-Dependent Constitutive Analysis of Hot Deformation and Hot Workability of T4-Treated ZK60 Magnesium Alloy[J]. Met. Mater, 2013, 4(9): 651-665.